Carbon Trends 5 (2021) 100123

Contents lists available at ScienceDirect

Carbon Trends

journal homepage: www.elsevier.com/locate/cartre

Graphene nanoplatelets can improve the performances of graphene oxide – polyaniline composite gas sensing aerogels

Filippo Pinelli, Tommaso Nespoli, Andrea Fiorati, Silvia Farè, Luca Magagnin, Filippo Rossi*

Department of Chemistry, Materials and Chemical Engineering "Giulio Natta", Politecnico di Milano, via Mancinelli 7, Milan 20131, Italy

ARTICLE INFO

Article history:
Received 29 August 2021
Revised 15 October 2021
Accepted 21 October 2021

Keywords:
Graphene
Conducting polymers
VOCs
Gas sensing
Graphene nanoplatelets
Aerogels

ABSTRACT

Aerogels are commonly regarded as soft and versatile materials for multiple applications thanks to their features such as elastic behavior, swelling ability and responsive characteristics. In the last decades these qualities have ensured them multiple uses in biomedical field as controlled drug delivery systems and scaffolds for tissue engineering applications. Recently their employment as sensors has attracted great interest especially thanks to their tunability and the possibility to be used as soft material instead of conventional and many times unreliable sensors in multiple sensing applications. In this work we synthetized graphene oxide/polyaniline aerogels by *in situ* chemical polymerization of aniline monomer in aqueous dispersion of graphene oxide sheets. We characterized the system through chemical and mechanical analysis, and we its responsivity as gas sensing device was verified. Moreover, we investigated the influence of the encapsulation of graphene nanoplatelets on the responsive ability of the device. The addition of the graphene moieties improves the conductivity of the system, its compressive mechanical resistance and the applicability of these devices as gas sensors.

1. Introduction

Aerogels are commonly identified as three-dimensional network made of polymeric chains, with unique features, including hydrophilicity, swelling behavior, softness, tunability and micro/nanosized pores [1,2]. The combination of these characteristics guarantees to aerogel networks great flexibility and the possibility to employ them in various fields such as drug delivery, tissue engineering and sensing applications [3–5]. Indeed one of the greatest characteristics of aerogels structures is their ability in responding to external stimuli thanks to their swelling behavior and great permeability that make them ideal candidates in sensing applications [5].

Despite the dissemination and the interest that nowadays aerogels have gained, conventional aerogels-based sensors still present in many cases limitations that restrict the range of their possible applications [6]. For example, certain aerogels formulations are mechanically weak, or they do not present considerable electrical conductivity or optical properties: this inevitably strongly restricts their possible engineering usages. Because of this, in the last two decades various strategies have been developed, in order to improve the characteristics of aerogels framework, such as the development of double network aerogel or the incorporation of nanocomposites moieties in the system [7,8]. A very interesting strategy in this context is represented by the possibility to synthetize graphene composite aerogel with the aim to combine the exceptional properties of graphene with the well-known features of aerogel framework [9]. In fact, graphene and graphene derivatives (e.g. graphene oxide) have been widely studied in combination with polymers for the synthesis of aerogel with enhanced properties, in term of mechanical behavior and electrical conductivity [10]. Graphene is commonly defined as a two-dimensional single layer of carbon atoms with a hexagonal structure and hybridized sp^2 orbitals. In this work we focused on graphene oxide (GO), which is usually obtained from graphite through oxidative exfoliation using strong oxidants and acids [11].

Because of this, GO is commonly characterized by structural defects in its orbital and functionalized with various groups such as epoxides or carboxylic groups.

The presence of these oxygen-containing groups favors the GO aqueous dispersion and make this compound suitable for combination with polymeric chains and aerogel synthesis [11,12]. As a consequence of this, various graphene-based materials reported in literature have been obtained working with GO [13]. In fact, its chemical structure guarantees in the final composite systems the

* Corresponding author.
E-mail address: filippo.rossi@polimi.it (F. Rossi).

https://doi.org/10.1016/j.cartre.2021.100123

presence of oxygenated functional groups and a hydrophobic basal plane which can represent the ideal substrate for molecular interactions with both small and big molecules. The proper combination of GO with polymeric chains or materials of different nature determine the possibility to exploit interactions of different nature (e.g. van der Waals, hydrophobic or electrostatic interactions) to encapsulate or capture specific molecules [14]. Moreover, in the context of interest of this work, it should be noted that in specific conditions, such as low pH, high GO concentration (> 4 mg/ml) and with large size GO sheets, GO can assemble to form a gel [15]. This can be obtained thanks to the reduction of repulsive forces between GO sheets obtained through the acid environment, where the carboxylic groups of GO become protonated and neutral. With the final aim to improve reproducibility and electrical conductivity together with mechanical properties we focused our attention to *in situ* polymerization of conductive aniline monomers in a GO solution to obtain gels (GO-PANI AG) [16]. The electrical characteristics of this kind of soft materials can be strongly influenced by their interactions with the external environment, especially in case of the presence of gas due to doping or dedoping process or adsorption of the molecule in the framework. Our aim was to obtain a final system with responsive characteristics when in contact with specific gaseous compounds. The interactions between the synthetized material and the gas and the subsequent response in its electrical behavior can be easily measured and used for gas detection. As reported in similar works already available in literature [16], the main limitation of the use of this soft materials in sensing applications resides in their poor mechanical properties that limits so their use.

In this direction here we studied the possibility to improve the aerogel performances encapsulating within the 3D network graphene nanoplatelets (GO-PANI AG + NPLS) that showed important improvement in the mechanical stability of the gel and were able to ameliorate its sensing features.

2. Materials and methods

2.1. Materials

Graphene oxide dispersion (10 mg/ml) was purchased from GOgraphene, trading name of William Blyte Limited (Harlow, Essex, England). The graphene oxide sheets were analyzed by the supplier through atomic force microscopy, the lateral dimensions measured were variable, with most sheets showing at least one lateral dimension greater than 5 µm. The sheet depth recorded was smaller than 2 nm, while for single graphene oxide sheets, the expected sheet depth is 1 nm, indicating that the graphene oxide analyzed here is no more than 2 sheets tall. Graphene nanoplatelets (purity: 99%, size: 3 nm) were bought from Nanografi Nanotechnology AS (Ankara, Turkey). Aniline and ammonium persulfate were bought from Sigma-Aldrich (Sigma-Aldrich Chemie GmbH, Deisenhofem, Germany). All other used chemicals were bought from Sigma-Aldrich (Sigma-Aldrich Chemie GmbH, Deisenhofem, Germany). The materials were used as received; solvents were of analytical grade.

2.2. Synthesis of graphene oxide-polyaniline composite aerogels

The composite aerogels made of graphene oxide and polyaniline were synthetized through *in situ* polymerization of aniline in GO dispersions [17]. Two different aqueous solutions were prepared: the aniline solution (100 μl/ml) was added dropwise in graphene oxide solution (7 mg/ml) to promote excellent mixing of the system. Then a solution of hydrochloric acid (1 ml, 1 M) was added to the system to promote the activation of aniline and finally ammonium persulfate, as oxidant agent, was added to guarantee the formation of the network. The aerogels were obtained through lyophilization and then characterized. Various ratio between aniline and graphene oxide were prepared and tested and employed (1:1, 1:2, 1:5); finally the optimal stability was obtained with the ratio 1:2.5.

2.3. Synthesis of graphene oxide-polyaniline composite aerogels with graphene nanoplatelets

The synthesis of graphene oxide-polyaniline composite aerogels with graphene nanoplatelets was obtained with a method similar to the one previously presented. Briefly, after the mixing of aniline solution (100 μl/ml) with graphene oxide one (7 mg/ml) and the addition of hydrochloric acid (1 ml, 1 M), graphene nanoplatelets (with a ratio 2:1 respect to graphene oxide) were added in the system under vigorous stirring to promote their homogenous dispersion.

Then after some minutes, ammonium persulfate was added to promote the formation of the framework with the encapsulation of the nanoplatelets inside it. The aerogels were obtained through lyophilization and then characterized.

2.4. Materials characterization

Various analyses and characterization were performed on the synthetized materials. First of all, the inner framework of the system was investigated with scanning electron microscope (SEM) together with X-ray diffraction (XRD). SEM analyses were realized using a Zeiss Evo50 with EDS Bruker Quantax 200, while XRD pattern were obtained with Philips X-ray diffractometer model PW1830 (Kα1Cu = 1.54058 Å). Moreover, the materials were chemically characterized with attenuated total reflection (ATR) analysis, using a Varian 640-IR spectrometer from Agilent Technologies. Spectra were collected at room temperature under dry nitrogen atmosphere in the 400–4000 cm-1 wavenumber range, with an average of 64 repetitive scans to guarantee a good signal-to-noise ratio and high reproducibility.

2.5. Mechanical analysis

In order to mechanically characterize the synthetized materials, we employed an Anton Paar MCR 702 TwinDrive Rheometer/DMA instrument, equipped with two parallel plate (50 mm lower L-PP50/TD/TS a 25 mm upper PP25) and a convection temperature device (CTD 180, Anton Paar). The tests were conducted on freeze-dried samples, with cylindrical shape (diameter = 9 mm, thickness = 5 mm). The samples were placed between the compression plates and a preload of 0.03 N was applied. Two different analyses were performed, at 20 °C: first of all, monotonic quasi-static uniaxial compression tests were carried out, applying a constant crosshead speed of 1 mm min^{-1} until a 70% strain was reached and compressive stress-strain curves were obtained. Then, the viscoelastic behavior of the materials was investigated in compression mode. During the test the sample was subjected to an oscillatory compression (frequency = 1 Hz) sweep, varying the strain in the range 0.1–10%. Storage and loss modulus trends were obtained from this test, so to evaluating the elastic and viscous contribution to the mechanical behavior of the materials under investigation.

2.6. Gas sensing tests

A small piece for each analyzed aerogel was fixed over interdigitated gold electrodes (Dropsens, Spain).

The whole system was left to rest for some minutes, monitoring its resistance value to verify the absence of significant variations, and then it was inserted in a cylindric chamber (approximately

400 cm^3 of volume) with gaseous cyclohexane, used as model of volatile organic compound, with a concentration of 1000 ppm. Gaseous phase of cyclohexane was obtained through the evaporation of the corresponding liquid compound. The resistance values were observed at different time points, and they have been plotted as normalized values respect to the initial value using the following formula:

$$NR_t = \frac{R_t - R_0}{R_0} \quad (5)$$

where NR_t represents the normalized value of the resistance at time t, R_t is the corresponding absolute value at time t and R_0 is the absolute value of resistance at the initial time. Various tests were conducted. First, we investigated the responsivity of the sensor in the first seconds of gas exposure. The sensor was exposed 30 s to gas and its electrical resistance value was continuously monitored to see its behavior in this initial phase. Then we investigate what happens to the sensor if we expose it for 5 min to gas and its response was measured at the end of this time span, then it was left in air to monitor the changes in its electrical parameters in this new condition after the exposure. Finally, a prolonged exposure of the sensor to gas was performed to investigate the behavior of the sensor when exposed for larger time to gas environment.

3. Results and discussion

3.1. Aerogels formation and characterization

As widely reported in literature, aniline can be easily polymerized through conventional chemical oxidative polymerization, working with a strong acid solution, and initiated by adding an oxidant (in this case ammonium persulfate) [18,19]. The redox reaction between aniline and APS guarantees the formation of aniline radicals that, in an acid environment, rearrange to form a para-coupled structure resulting in an emeraldine salt, characteristic of polyaniline [20]. The acidic environment is in this case pivotal to promote the acid doping process of polyaniline which is the key element to obtain the conductive form of the polymer. If the polymerization is carried out in a concentrated graphene oxide dispersion, as the case of the present work, an aerogel can be formed with polyaniline that is arranged between the sheets of graphene and guarantees the formation of the three-dimensional network. In fact, GO sheets are widely recognized as 2D polyelectrolytes, with negative charges at their edges and defects on their basal planes [9]. Because of this, during polymerization the nucleation of positively charged PANI chains take place on the surface of GO sheets and this process weakens the electrostatic repulsion force of the graphene oxide moieties. The addition of graphene nanoplatelets occur before the addition of the oxidant, so that they are dispersed in the solution and the gelification process guarantees their encapsulation inside the framework. In Fig. 1 we reported the schematization of the synthesis of the aerogels (a) as reported in Materials and Methods section together with the chemical structure of the framework (b) and an example of the gel layer over the interdigitated electrode (c). Considering GO-PANI framework, the carboxyl groups of graphene oxide sheets react with the chains of polyaniline, resulting in the formation of the 3D network. In fact, as already mentioned, the gelification process is favored by the positive charges of polyaniline, that reduce the negative charges of the oxygenated groups of the graphene and by the possible formation of aerogen bonds and π-π bonds in the structure.

SEM analyses of the lyophilized aerogels confirmed the formation of a porous framework without the presence of observable particles (Fig. 2). Moreover, the inner structure of the gel is not significantly modified by the presence of the graphene nanoplatelets. Indeed, no observable differences are visible comparing GO-PANI AG (Fig. 2A, B) with GO-PANI AG + NPLS (Fig. 2C, D) underlining the good dispersion of all the components within the networks.

The two aerogels formulations were then characterized through ATR-FTIR analysis and XRD. In the Fig. 3(a), we reported the spectra (transmittance [%] versus wavenumber [cm^{-1}]) of graphene nanoplatelets (NPLS), polyaniline aerogels (PANI AG), polyaniline – graphene oxide aerogels (GO-PANI AG) and polyaniline – graphene oxide aerogels with graphene nanoplatelets (GO-PANI AG + NPLS). Characteristics of the spectra of PANI and of graphene nanoplatelets can be distinguished in the spectra of GO-PANI aerogels with slight variations in intensity and a shift towards higher wavenumber due to the interaction between PANI and GO.

This can be observed especially for peaks at ~1423 cm^{-1}, attributed to $C = N$ stretching mode of vibration of quinoid units, at ~1100 cm^{-1}, that is attributed to B-NH^+=Q stretching (where B represent the benzenoid ring and Q the quinoid ring) and that is a measure of the degree of delocalization of electrons, at ~956 cm^{-1} and ~840 cm^{-1}, related to C–H stretching. An increase in the intensity of the peak at ~1100 cm^{-1} was observed in the composite material, possibly caused by the interaction between the π bonded structure of GO and the conjugated structure of PANI [21]. An additional wide band for the composite material is observed between 3000 and 3400 cm^{-1} due to the O–H functional groups of graphene oxide. Furthermore, we characterized the materials using the XRD technique as reported in Fig. 3(b). The two composite materials showed very similar profiles, with a repeated and similar crystalline structure where the addition of graphene nanoplatelets does not change the framework of the system. From XRD spectra the presence of organic and inorganic phases are well visible.

In particular $2\theta = 23.7$ ° is assigned to the (200) planes of emeraldine form of PANI. The high peak at $2\theta = 23.7$ ° and the almost disappeared peak at $2\theta = 24.7$ ° show that GO sheets are uniformly coated with PANI network [22]. Furthermore, around $2\theta = 26$ ° it is possible to observe the signal related to graphene associated with the addition of graphene nanoplatelets [23,24].

3.2. Mechanical analysis of the materials

Lyophilized GO-PANI AG and GO-PANI + NPLS AG were mechanically analyzed. Compression mechanical tests were performed between 0 and 70% strain and the compressive stress-strain curves are reported in Fig. 4(a). Both the profiles exhibit the typical trend for porous materials: in the initial region of the curve a confined elastic deformation region can be identified with the subsequent plastic deformation region, also defined as densification region [25]. This behavior can be explained considering the progressive collapsing of the internal porous structure of the material due to the compression of the specimen that led to a densification of the porous structure. Then, it can be observed a higher increase in the stress for GO-PANI + NPLS AG compared to GO-PANI AG, after the densification region of the curve. In fact, when the sample is completely densified, the material exhibits the behavior of a non-porous material.

Comparing the two different formulations, it is well evident how the presence of graphene nanoplatelets inside the framework can guarantee an improvement in the compressive mechanical behavior of the material [26,27].

Graphene oxide-aniline aerogels and the formulation functionalized with graphene nanoplatelets were characterized with an oscillatory test, the amplitude sweep. During the test, the deformation amplitude is varied while the frequency is maintained constant [28]. Two parameters were investigated, the elastic or storage modulus of a material, concerning the elastic contribution of the material, and the loss modulus, related to the viscous contribution to the whole mechanical behavior of the investigated materials [29]. These parameters allow first to determine the limit of

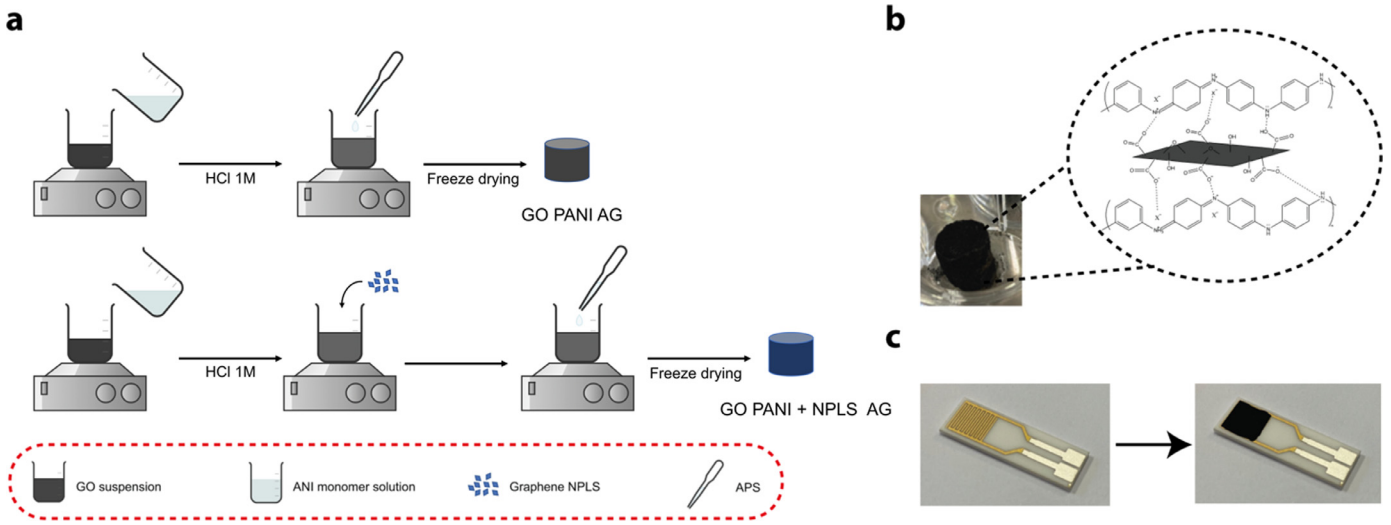

Fig. 1. (a) Schematic representation of the synthesis procedure for GO-PANI aerogel (upper scheme) and GO-PANI + NPLS aerogels (lower scheme). (b) Schematization of the gel formation between polyaniline chains and graphene oxide sheets (black plane) (c) Representation of the gel framework over the interdigitated gold electrode.

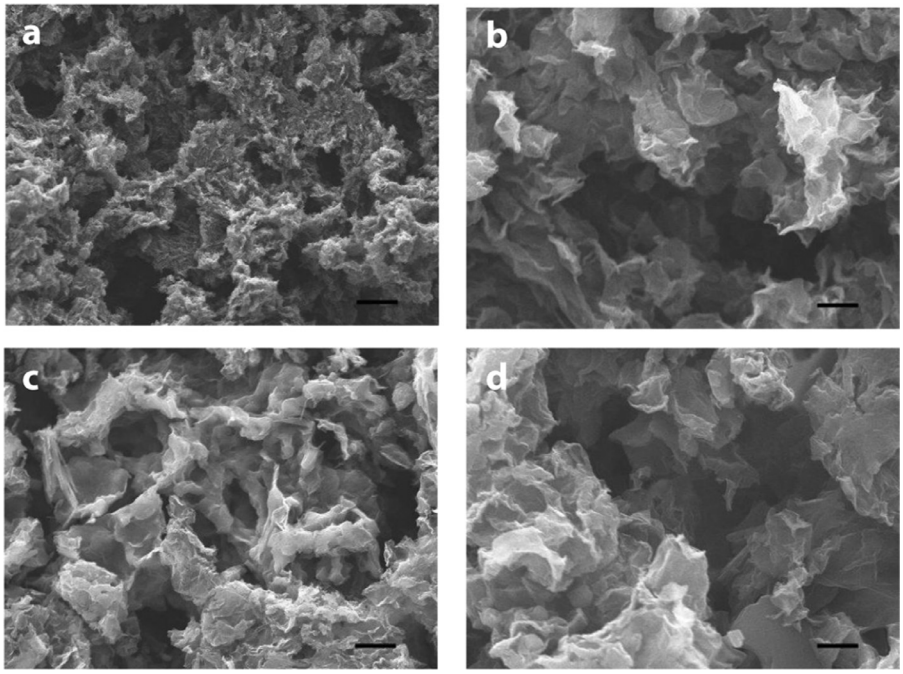

Fig. 2. SEM images of the lyophilized graphene oxide – polyaniline aerogels (a) and (b) and of graphene oxide – polyaniline aerogels with graphene nanoplatelets (c) and (d). Scale bars:(a) and (c) 10 μm, (b) and (d) 2 μm.

the linear viscoelastic region (LVE region). The LVE region indicates the range in which the E' and E'' trends exhibit a linear behavior, whereas, after the LVE region a non-linear viscoelastic behavior is observed. Moreover if $E' > E''$ in the LVE region the elastic contribution to the mechanical behavior of the material is higher than the viscous one, while the opposite case concerns the preponderant contribution of the viscous behavior over the elastic one [28,30].

Considering the E' and E'' trends reported in Fig. 4(b), both of the investigated materials present $E' > E''$ in the LVE region, as expected. Moreover, it is well evident how the LVE region for the GO-PANI AG is wider respect to the one of GO-PANI + NPLS AG. The contribution of graphene nanoplatelets in the compressive mechanical behavior of the obtained porous structure is evident by fact that the compressive mechanical strength improved compared to the GO-PANI AG structures and by DMA it is observable a decreasing in the E' values when the strain increases caused by the higher stiffness of the structure. The viscous contribution to the mechanical behavior of both the investigated structures is very similar, as evidenced by the lower values compared to the E' ones, and the constant behavior when the strain is increased.

3.3. Gas sensing results

Various scientific works report the use of conducting polymers (CPs) as building material to fabricate gas sensors, thanks to their ability in changing some features, especially electrical properties, through the chemical or physical interactions with various molecules [31,32]. It is well known how higher surface area of the employed sensing material, together with reduced thickness of the

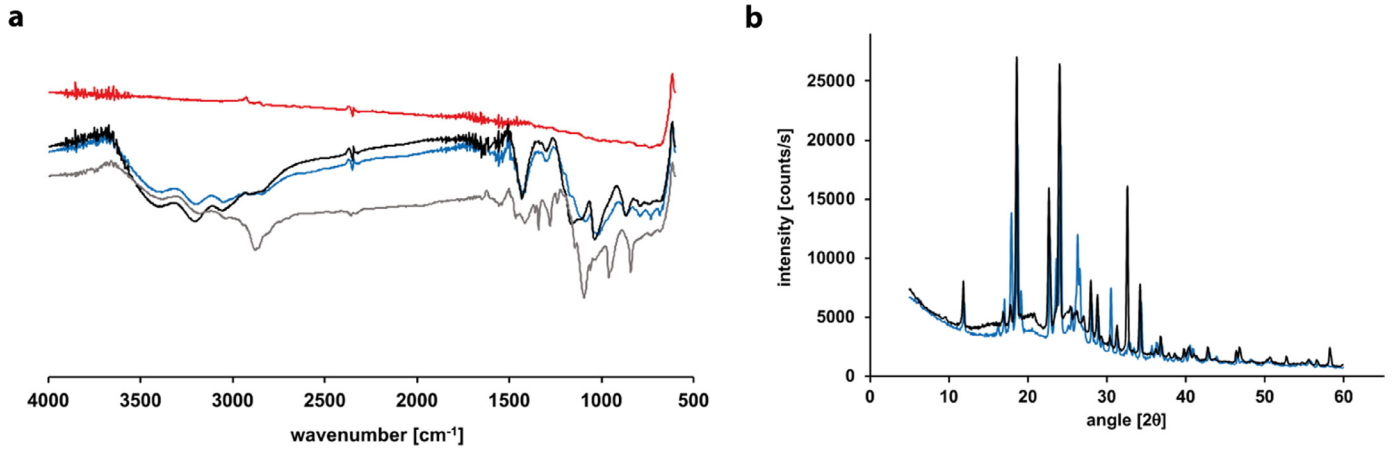

Fig. 3. (a) ATR – FTIR spectra of NPLS (red line), PANI AG (gray line), GO-PANI AG (black line) and GO-PANI + NPLS AG (blue line). (b) XRD pattern of GO-PANI AG (black line) and GO-PANI + NPLS AG (blue line) (For interpretation of the references to color in this figure legend, the reader is referred to the web version of this article.).

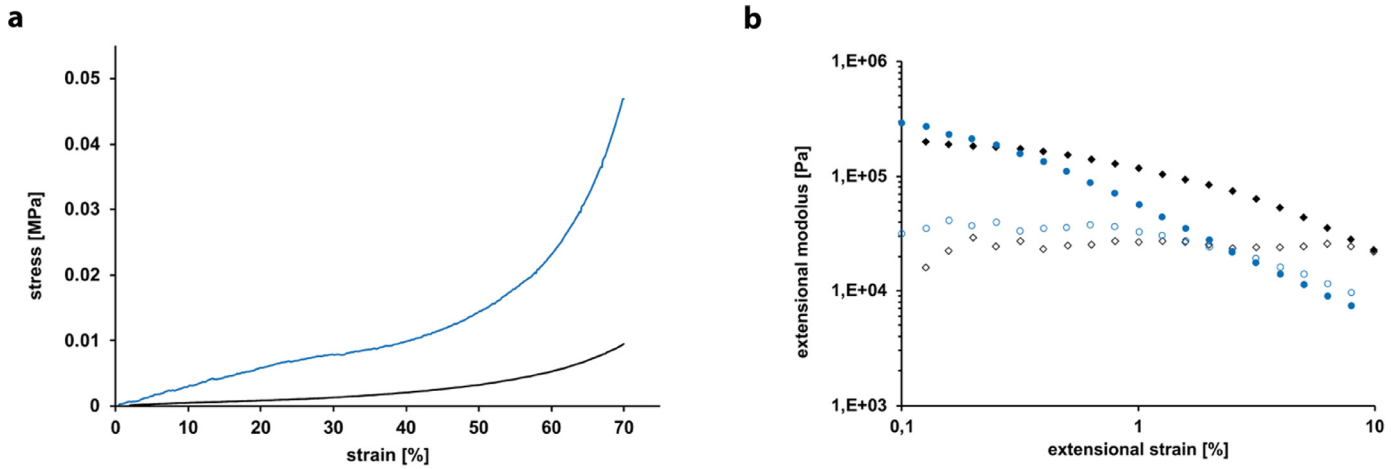

Fig. 4. (a) Compressive stress-strain curves of the GO-PANI AG (black line) and GO-PANI + NPLS AG (blue line). (b) Amplitude sweep tests results of the GO-PANI AG (black rhombuses) and GO-PANI + NPLS AG (blue spheres). The storage modulus (E') trends are reported with the filled dots, while the loss modulus (E'') ones with the hollow ones (For interpretation of the references to color in this figure legend, the reader is referred to the web version of this article.).

whole system, can guarantee higher sensitivity because of a better diffusion process of the analyte inside the framework [33]. In the present work we employed lyophilized conducting polymer composite aerogels as sensing materials with very reduced dimensions in the order of 1 mm of thickness. The lyophilized structures of the gels resemble the ones of aerogels and the SEM analyses confirmed the porosity of the network that is essential for good interactions between the system and the gas. As already discussed, in this work we compare the behavior and the response in a cyclohexane environment of two aerogels formulations, reported in the previous section, to investigate the influence of the encapsulation of graphene nanoplatelets inside the framework of the gel on the responsive ability of these materials.

It is well known how the electrical conductivity of conducting polymers and their composites, including polyaniline, depend upon doping agents and protonation of the moieties of the materials [34]. As previously discussed, in this work we adopted the acid doping process to obtain the emeraldine salt form of PANI. This process determines a structural change on the material, with one pair unpaired spin per repeat unit without any alter in the number of the electrons caused by proton induced spin unpaired mechanism [34]. Moreover, any doping or dedoping process, defined as the act of adding or removing impurity to a material, taking place on the analyzed frameworks can determine an alteration of the electrical properties of the system. In this case the response that can be observed after the exposure to gas of these materials can be explained with a doping process on the framework of the system. In fact composite GO/polymer aerogel and aerogel have been reported as valuable gas adsorbents thanks to their porous structure [35,36]. In addition, the system functionalized with nanoplatelets shows enhanced sensitivity with an amplified response in the same time interval. These results are reported in Fig. 5, where we compared the polyaniline-graphene oxide aerogels and the formulation functionalized with graphene nanoplatelets. In Fig. 5(a) we reported the focus of the response of the sensors in the first 30 s of exposure to gas (range 10–40 s in the plot) which are for sure the most important for the sensitivity of the device. We observed, from this continuous analysis, the jump of the normalized electrical resistance values which is clearly more intense for GO-PANI + NPLS AG. The same behavior is noticeable in Fig. 5(b) during the 5 min test, where an increase of the electrical resistance variation up to 20% for GO-PANI G and 40% for GO-PANI + NPLS AG is visible together with their subsequent stabilization when exposed to air. On the other hand, in Fig. 5(c) the results of the prolonged exposure of the sensor to gas are reported and even in this case the GO-PANI + NPLS AG presented higher responsivity and higher values of normalized electrical variations were measured.

In all the cases the higher responsivity of graphene oxide – polyaniline aerogels with graphene nanoplatelets is clearly visible.

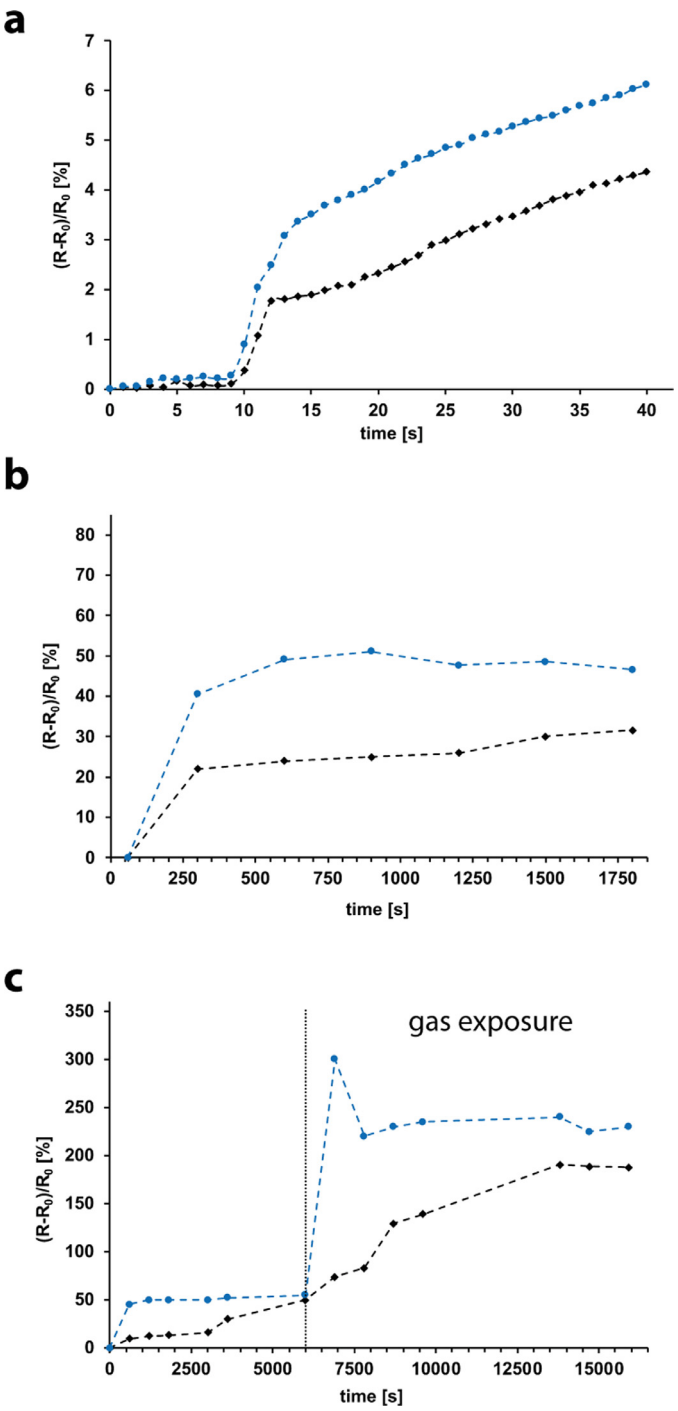

Fig. 5. Normalized electrical resistance of (a) GO-PANI AG (black line) and GO-PANI + NPLS AG (blue line) respect to time during the first 30 s of exposure to gas (time span 10–40 s) (b) GO-PANI AG (black line) and GO-PANI + NPLS AG (blue line) respect to time after 5 min exposure to gas and subsequent rest in air (c) GO-PANI AG (black line) and GO-PANI + NPLS AG (blue line) respect to time during prolonged exposure of the materials to gas (For interpretation of the references to color in this figure legend, the reader is referred to the web version of this article.).

This behavior can be justified considering the improvement in the electrical properties of the system due to the presence of graphene nanoplatelets which are well known conductors [26,27]. The improvement in the conductivity of the system, without varying the ratio between graphene oxide and aniline, is extremely useful in enhancing the response of the sensor thanks to higher values of the normalized resistance in face of constant inner framework of the device.

Moreover, during the adsorption of the gas on the composite material, a localize swelling could occur, which can separate the dispersed nanoplatelets in the framework, resulting in an increase in the electrical resistance [37]. In the Fig. 5 it is well evident how both materials exhibit the biggest change in the first 300–40 s, confirming the responsivity of the material and the hypothesis of the contribution of a doping process in the behavior of the system.

4. Conclusion

In this work we successfully synthetized and characterized polyaniline-graphene oxide aerogels and we functionalized them through the encapsulation inside the polymeric network of graphene nanoplatelets. These devices were mechanically analyzed and their sensitivity as gas sensor devices has been investigated, confirming the potential of these formulations and the improvement that can be achieved working with more graphene moieties in the system both in term of sensing ability and for mechanical characteristics. Because of the results obtained, one of the possible applications of these devices could be for example as end of the service life indicator of the respirator cartridges commonly employed in the protection of workers from gas exposure.

Declaration of Competing Interest

The authors declare that they have no known competing financial interests or personal relationships that could have appeared to influence the work reported in this paper.

Supplementary materials

Supplementary material associated with this article can be found, in the online version, at doi:10.1016/j.cartre.2021.100123.

References

[1] M. Mahinroosta, Z. Jomeh Farsangi, A. Allahverdi, Z. Shakoori, Hydrogels as intelligent materials: a brief review of synthesis, properties and applications, Mater. Today Chem. 8 (2018) 42–55, doi:10.1016/j.mtchem.2018.02.004.
[2] E.M. Ahmed, Hydrogels : introduction, preparation, characterization and applications: a review, J. Adv. Res. 6 (2015), doi:10.1016/j.jare.2013.07.006.
[3] F. Ullah, M.B.H. Othman, F. Javed, Z. Ahmad, H.M. Akil, Classification, processing and application of hydrogels: a review, Mater. Sci. Eng. C 57 (2015) 414–433, doi:10.1016/j.msec.2015.07.053.
[4] S. Geng, H. Zhao, G. Zhan, Y. Zhao, X. Yang, Injectable *in situ* forming hydrogels of thermosensitive polypyrrole nanoplatforms for precisely synergistic photothermo-chemotherapy, ACS Appl. Mater. Interfaces 12 (2020) 7995–8005, doi:10.1021/acsami.9b22654.
[5] F. Pinelli, L. Magagnin, F. Rossi, Progress in hydrogels for sensing applications: a review, Mater. Today Chem. 17 (2020) 100317, doi:10.1016/j.mtchem.2020.100317.
[6] X. Hu, R. Liang, J. Li, Z. Liu, G. Sun, Mechanically strong hydrogels achieved by designing homogeneous network structure, Mater. Des. 163 (2019) 107547, doi:10.1016/j.matdes.2018.107547.
[7] Q. Chen, H. Chen, L. Zhu, J. Zheng, Fundamentals of double network hydrogels, J. Mater. Chem. B 3 (2015) 3654–3676, doi:10.1039/C5TB00123D.
[8] F. Pinelli, L. Magagnin, F. Rossi, Can nanostructures improve hydrogel-based biosensors performance ? Nanomedicine 16 (2021) 681–683, doi:10.2217/nnm-2021-0053.
[9] G. Liao, J. Hu, Z. Chen, R. Zhang, G. Wang, T. Kuang, Preparation, properties, and applications of graphene-based hydrogels, Front. Chem. 6 (2018) 1–5, doi:10.3389/fchem.2018.00450.
[10] J. Yi, G. Choe, J. Park, J.Y. Lee, Graphene oxide-incorporated hydrogels for biomedical applications, Polym. J. 52 (2020) 823–837, doi:10.1038/s41428-020-0350-9.
[11] Z. Tan, S. Ohara, H. Abe, M. Naito, Synthesis and processing of graphene hydrogels for electronics applications, RSC Adv. 4 (2014) 8874–8878, doi:10.1039/C3RA46856A.
[12] H. Lu, S. Zhang, L. Guo, W. Li, Applications of graphene-based composite hydrogels: a review, RSC Adv. 7 (2017) 51008–51020, doi:10.1039/c7ra09634h.
[13] A.T. Smith, A.M. LaChance, S. Zeng, B. Liu, L. Sun, Synthesis, properties, and applications of graphene oxide/reduced graphene oxide and their nanocomposites, Nano Mater. Sci. 1 (2019) 31–47, doi:10.1016/j.nanoms.2019.02.004.

[14] H.P. Cong, P. Wang, S.H. Yu, Stretchable and self-healing graphene oxide-polymer composite hydrogels: a dual-network design, Chem. Mater. 25 (2013) 3357–3362, doi:10.1021/cm401919c.
[15] K. SHENG, Y. XU, C. LI, G. SHI, High-performance self-assembled graphene hydrogels prepared by chemical reduction of graphene oxide, New Carbon Mater. 26 (2011) 9–15, doi:10.1016/S1872-5805(11)60062-0.
[16] M. Tomczykowa, M.E. Plonska-Brzezinska, Conducting polymers, hydrogels and their composites: preparation, properties and bioapplications, Polymers 11 (2019) 1–36 (Basel), doi:10.3390/polym11020350.
[17] X. Li, Q. Zhong, X. Zhang, T. Li, J. Huang, *In-situ* polymerization of polyaniline on the surface of graphene oxide for high electrochemical capacitance, Thin Solid Films 584 (2015) 348–352, doi:10.1016/j.tsf.2015.01.055.
[18] S.J. Tang, A.T. Wang, S.Y. Lin, K.Y. Huang, C.C. Yang, J.M. Yeh, K.C. Chiu, Polymerization of aniline under various concentrations of APS and HCl, Polym. J. 43 (2011) 667–675, doi:10.1038/pj.2011.43.
[19] N.Y. Abu-Thabit, Chemical oxidative polymerization of polyaniline: a practical approach for preparation of smart conductive textiles, J. Chem. Educ. 93 (2016) 1606–1611, doi:10.1021/acs.jchemed.6b00060.
[20] B. Yan, Z. Chen, L. Cai, Z. Chen, J. Fu, Q. Xu, Fabrication of polyaniline hydrogel: synthesis, characterization and adsorption of methylene blue, Appl. Surf. Sci. 356 (2015) 39–47, doi:10.1016/j.apsusc.2015.08.024.
[21] M. Mitra, C. Kulsi, K. Chatterjee, K. Kargupta, S. Ganguly, D. Banerjee, S. Goswami, Reduced graphene oxide-polyaniline composites - synthesis, characterization and optimization for thermoelectric applications, RSC Adv. 5 (2015) 31039–31048, doi:10.1039/c5ra01794g.
[22] L. Zhang, Z. Zhang, Y. Lv, X. Chen, Z. Wu, Y. He, Y. Zou, Reduced graphene oxide aerogels with uniformly self-assembled polyaniline nanosheets for electromagnetic absorption, ACS Appl. Nano Mater. 3 (2020) 5978–5986, doi:10.1021/acsanm.0c01115.
[23] A. Maniadi, M. Vamvakaki, M. Suchea, I.V. Tudose, M. Popescu, C. Romanitan, C. Pachiu, O.N. Ionescu, Z. Viskadourakis, G. Kenanakis, E. Koudoumas, Effect of graphene nanoplatelets on the structure, the morphology, and the dielectric behavior of low-density polyethylene nanocomposites, Materials 13 (2020) 1–12 (Basel), doi:10.3390/ma13214776.
[24] Q. Cheng, Y. Okamoto, N. Tamura, M. Tsuji, S. Maruyama, Y. Matsuo, Graphene-like-graphite as fast-chargeable and high-capacity anode materials for lithium ion batteries, Sci. Rep. 7 (2017) 1–14, doi:10.1038/s41598-017-14504-8.
[25] S. Ja-Ye, S. Do-Sik, Compressive behavior of porous materials fabricated by laser melting deposition using AlSi12 powder and foaming agent, Mater. Res. Express 6 (2019), doi:10.1088/2053-1591/aafc5a.
[26] X. Jiang, L.T. Drzal, Improving electrical conductivity and mechanical properties of high density polyethylene through incorporation of paraffin wax coated exfoliated graphene nanoplatelets and multi-wall carbon nano-tubes, Compos. Part A Appl. Sci. Manuf. 42 (2011) 1840–1849, doi:10.1016/j.compositesa.2011.08.011.
[27] M. Monti, M. Rallini, D. Puglia, L. Peponi, L. Torre, J.M. Kenny, Morphology and electrical properties of graphene-epoxy nanocomposites obtained by different solvent assisted processing methods, Compos. Part A Appl. Sci. Manuf. 46 (2013) 166–172, doi:10.1016/j.compositesa.2012.11.005.
[28] H. Meeuw, V.K. Wisniewski, B. Fiedler, Frequency or amplitude? Rheo-electrical characterization of carbon nanoparticle filled epoxy systems, Polymers 10 (2018) 1–16 (Basel), doi:10.3390/polym10090999.
[29] F. Cuomo, M. Cofelice, F. Lopez, Rheological characterization of hydrogels from alginate-based nanodispersion, Polymers 11 (2019) (Basel), doi:10.3390/polym11020259.
[30] S. Minami, D. Suzuki, K. Urayama, Rheological aspects of colloidal gels in thermoresponsive microgel suspensions: formation, structure, and linear and nonlinear viscoelasticity, Curr. Opin. Colloid Interface Sci. 43 (2019) 113–124, doi:10.1016/j.cocis.2019.04.004.
[31] H. Bai, K. Sheng, P. Zhang, C. Li, G. Shi, Graphene oxide/conducting polymer composite hydrogels, J. Mater. Chem. 21 (2011) 18653–18658, doi:10.1039/c1jm13918e.
[32] Y. Wang, A. Liu, Y. Han, T. Li, Sensors based on conductive polymers and their composites: a review, Polym. Int. 69 (2020) 7–17, doi:10.1002/pi.5907.
[33] H. Bai, G. Shi, Gas sensors based on conducting polymers, Sensors 7 (2007) 267–307, doi:10.4018/978-1-5225-1798-6.ch022.
[34] M. Beygisangchin, S.A. Rashid, S. Shafie, A.R. Sadrolhosseini, H.N Lim, Preparations, properties, and applications of polyaniline and polyaniline thin films-A review, Polymers 13, MDPI, 2021.
[35] Z.Y. Sui, Y. Cui, J.H. Zhu, B.H. Han, Preparation of three-dimensional graphene oxide-polyethylenimine porous materials as dye and gas adsorbents, ACS Appl. Mater. Interfaces 5 (2013) 9172–9179, doi:10.1021/am402661t.
[36] O.C. Compton, S. Kim, C. Pierre, J.M. Torkelson, S.T. Nguyen, Crumpled graphene nanosheets as highly effective barrier property enhancers, Adv. Mater. 22 (2010) 4759–4763, doi:10.1002/adma.201000960.
[37] M.S. Wiederoder, M. Weiss, B. Yoon, R.C. Paffenroth, S.K. McGraw, J.R. Uzarski, Impact of graphene nanoplatelet concentration and film thickness on vapor detection for polymer based chemiresistive sensors, Curr. Appl. Phys. 19 (2019) 978–983, doi:10.1016/j.cap.2019.05.011.